Optical Materials 98 (2019) 109495

Contents lists available at ScienceDirect

Optical Materials

journal homepage: http://www.elsevier.com/locate/optmat

The effect of doping and annealing on the nonlinear absorption characteristics in hydrothermally grown Al doped ZnO thin films

Yasemin Pepe [a], Mehmet Ali Yildirim [b], Ahmet Karatay [a,*], Aytunc Ates [c], Huseyin Unver [d], Ayhan Elmali [a,**]

[a] Department of Engineering Physics, Faculty of Engineering, Ankara University, 06100, Beşevler, Ankara, Turkey
[b] Department of Electric and Electronics Engineering, Engineering Faculty, Erzincan University, Erzincan, Turkey
[c] Department of Material Engineering, Engineering and Natural Sciences Faculty, Yıldırım Beyazıt University, Ankara, Turkey
[d] Department of Physics, Faculty of Science, Ankara University, 06100, Beşevler, Ankara, Turkey

ARTICLE INFO

Keywords:
Hydrothermal grown
Al doped ZnO
Amorphous semiconductor
Nonlinear absorption
Defect states

ABSTRACT

The effects of annealing and Al dopant on the nonlinear absorption characteristics of amorphous ZnO thin films were studied experimentally and theoretically. The structural patterns of AZO thin films grown at various growth temperatures (80°C, 90°C, 100°C) and Al doping ratios (%5, %10, %20) were determined by using x-ray diffraction. The results revealed that the crystallinity increased with increasing growth temperature and Al doping ratio. The optical band gap decreased from 3.91 to 3.78 eV and the transmittance of AZO thin films decreased from 90% to 55% with increasing Al molar ratio. The open aperture Gaussian beam Z-scan measurements indicated that all studied films exhibited nonlinear absorption behavior due to the defect states inside energy bandgap. The nonlinear absorption coefficients increased from 1.34×10^{-4} to 6.12×10^{-4} cm/W for 4 ns pulse duration with increasing of doping concentration. The experimental curves were fitted to the theory of open aperture Gaussian beam Z-scan based on the Adomian decomposition method to obtain nonlinear absorption coefficients along with saturation intensity thresholds. In order to investigate the effect of free carrier absorption, the OA Z-scan experiments were also performed for 65 ps pulse duration. The nonlinear absorption coefficients were found to be 0.58×10^{-4}, 1.81×10^{-4} and 3.29×10^{-4} cm/W for 65 ps pulse duration. For nanosecond pulse durations, the obtained nonlinear absorption coefficient values of thin films are bigger than the values of picosecond pulse durations due to the greater contribution of free carrier absorption. Increasing annealing temperature from 100°C to 400°C leads to decreasing nonlinear absorption coefficients owing to decreasing localized defect states.

1. Introduction

Nonlinear optical properties of semiconductors have been studied extensively because of scientific interests and their potential usage in technological applications. Recently, nonlinear absorption (NA) and saturable absorption (SA) characteristics of amorphous semiconductor thin films were investigated using experimental and theoretical studies [1–3]. These studies revealed that thinner films exhibit saturable absorption while thicker films exhibit nonlinear absorption. The observed NA and SA characteristics depending on the film thickness can be attributed to the localized defect states which increase significantly as the film thickness increases. These localized defect states can be filled by one photon, two photon, and free carrier mechanisms. Filling the localized defect states causes SA behavior. In the light of the previous works, the goal of this work is to attempt to study the effects of both Al doping and annealing on nonlinear absorption characteristics of ZnO thin films experimentally and theoretically. Since there are a lot of localized defect states in energy bandgap of amorphous semiconductors due to the loss of long-range order and defects such as dangling bonds and impurities, semiconductor with wide direct bandgap is more suitable choice to see the effect of doping and annealing.

It is well known that by adding the impurities to a semiconductor of wide energy band gap leads to modify the optoelectrical and nonlinear characteristics intensely [4–6]. ZnO has a wide direct bandgap (3.37 eV)

* Corresponding author.
** Corresponding author.
E-mail addresses: akaratay@eng.ankara.edu.tr (A. Karatay), elmali@eng.ankara.edu.tr (A. Elmali).

https://doi.org/10.1016/j.optmat.2019.109495
Received 25 June 2019; Received in revised form 24 September 2019; Accepted 29 October 2019
Available online 6 November 2019
0925-3467/© 2019 Elsevier B.V. All rights reserved.

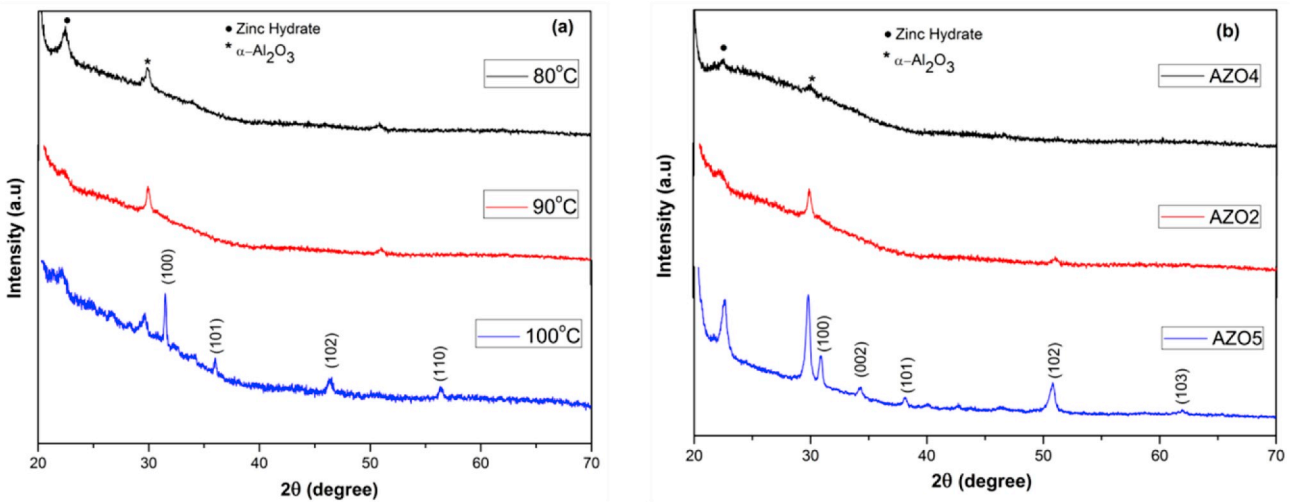


Fig. 1. XRD spectra of AZO thin films at (a) 80 °C, 90 °C, 100 °C growth temperature and (b) %5 (AZO4), %10 (AZO2), %20 (AZO5) Al doping ratios.

and a large exciton binding energy (60 meV) at room temperature [7,8]. ZnO is widely investigated for technical importance as field emitters [9], field effect transistors [10], dye-sensitized solar cells [11], photodetectors [12], gas sensors [13] and other optoelectronic devices [14,15]. The various elements were used as dopants such as Mn, Al, In, Mg, Ga and Ni to improve the optical and electrical properties of ZnO [16–19]. Among these elements, Al is a promising dopant due to the smaller ionic radious of Al^{3+} (0.54 Å) than the ionic radious of Zn^{2+} (0.74 Å). Therefore, Al^{3+} ion replaces Zn^{2+} ion into ZnO crystal lattice and it changes the electrical, optical and nonlinear optical properties of ZnO by creating stresses and defects.

The various deposition methods such as chemical vapor deposition, molecular beam epitaxy, spray pyrolysis, magnetron sputtering, sol-gel process, electron beam evaporation, hydrothermal method, atomic layer deposition and pulsed laser deposition were used to synthesis of Al doped ZnO thin films [20–28]. Among these methods, hydrothermal method is a low-cost, simplicity and high efficiency method. Recently, the absorption and emission properties of Al:ZnO nanostructures grown by hydrothermal method [29], electrical, linear and nonlinear optical properties of Al doped ZnO thin films prepared by laser ablation method [30], nonlinear optical properties of Al doped ZnO fabricated using spray pyrolysis deposition method [31], the nonlinear optical properties of Al:ZnO and Li:ZnO thin films by sol-gel spin coating method [32] were investigated. More recently, G. P. Bharti et al. investigated the Al incorporation on nonlinear optical properties in ZnO thin films prepared by pulse laser deposition [33]. To the best of our knowledge, till now, there has been no major study describing the effect of both doping and the annealing on nonlinear optical properties of hydrothermally grown AZO thin films taking into account one photon, two photon and free carrier absorptions. In this study, Al doped ZnO thin films with 5%, 10% and 20% were grown on glass substrates at various growth temperatures such as 80°C, 90°C and 100°C by using hydrothermal method. Al doped ZnO films were annealed at 100°C, 200°C, 300°C and 400°C. We investigated the NA and SA properties with open aperture (OA) Z-scan technique at 532 nm for 4 ns and 65 ps pulse durations.

2. Experimental

2.1. Preparation of AZO thin films

Hydrothermal synthesis has many advantages over other synthesis process. Compared to other methods, the respective costs for energy, precursors and instrumentation are much lower in the hydrothermal method. In this work, zinc nitrate tetrahydrate [$Zn(NO_3)_2{\cdot}4H_2O$], hexamethylenetetramine (HMT –$C_6H_{12}N_4$) and aluminum chloride ($AlCl_3$) were used as precursor materials. The aqueous solutions of 0.03 M $Zn(NO_3)_2{\cdot}4H_2O$, 0.03 M $C_6H_{12}N_4$ and 0.03 M $AlCl_3$ were prepared separately using 30 ml deionized water. The 0.03 M $Zn(NO_3)_2{\cdot}4H_2O$ and 0.03 M $C_6H_{12}N_4$ solutions were slowly mixed stirring (180 rpm) until complete dissolution. Then, final solution with different Al/Zn molar ratios of $Al^{3+}/Zn^{3+} = 5\%$, 10%, 20%; were prepared by adding appropriate proportions 0.03 M $AlCl_3$ solution to the mixture solution prepared for AZO films. The pH value of the final solution was adjusted to pH = 7. After that the final solution was transferred into a Teflon-lined stainless steel autoclave where glass substrate was placed. The growth was carried out by maintaining the temperature of the autoclave at 80°C, 90°C and 100°C for 12 h, separately. Al doping ratio was kept constant at 10% for 80°C, 90°C and 100°C growth temperatures. Also, the growth temperature and growth time for analysis of the Al doping effect were kept constant at 90°C and 12 h, respectively. After the growth, the substrates were rinsed with deionized water and dried in air at room temperature. The thin films were named as AZO1, AZO2 and AZO3 for 10% Al doped AZO thin films grown at 80°C, 90°C and 100°C growth temperatures, respectively. The thin films were named as AZO4, AZO2 and AZO5 for 5% Al doped AZO, 10% Al doped AZO and 20% Al doped AZO thin films grown at 90°C growth temperature, respectively.

2.2. Structural and optical characterization

The structural analysis of the films were carried out by using x-ray diffraction (XRD) technique varying the diffraction angle 20° to 70° range using CuKα radiation. The optical absorption and transmission measurements of AZO thin films were performed by using UV–vis spectrophotometer (Shimadzu UV-1800). The spectroscopic ellipsometer (Woollam,-M2000V) in the photon energy range from 1.24 to 3.34 eV was used to determine the film thicknesses. The three angles of incidences (65°, 70° and 75°) were used to in thickness measurements to increase the fitting accuracy. The film thicknesses were found to be about 300 nm for all films. NA of amorphous films were measured by using OA *Z*-scan technique as described in the literature. Two laser sources with nanosecond and picosecond pulse durations were used for the OA Z-scan experiments (1:Q-switched Nd:YAG laser with 4 ns pulse duration, 532 nm wavelength and 10 Hz repetition rate, 2: Q-switched Nd:YAG laser with 65 ps pulse duration, 532 nm wavelength and 10 Hz repetition rate). The AZO films were annealed at 100°C, 200°C, 300°C and 400°C for 3 min in air atmosphere.

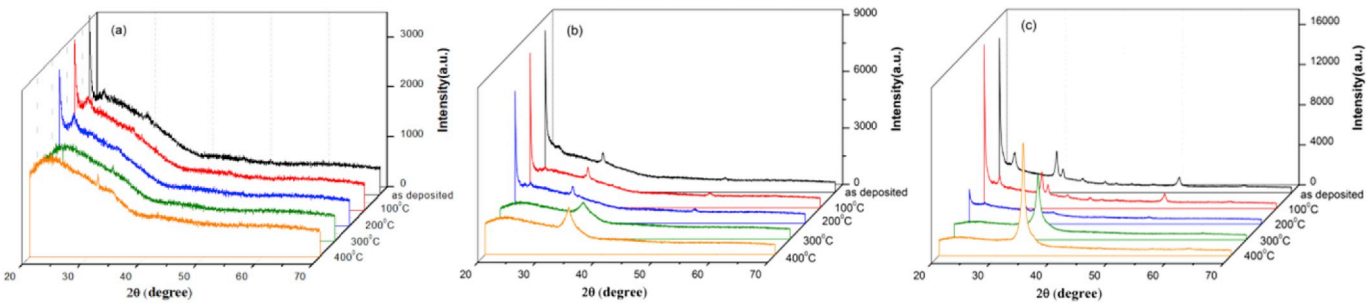


Fig. 2. XRD spectra of as-grown and annealed (a) AZO4, (b) AZO2 and (c) AZO5 thin films.

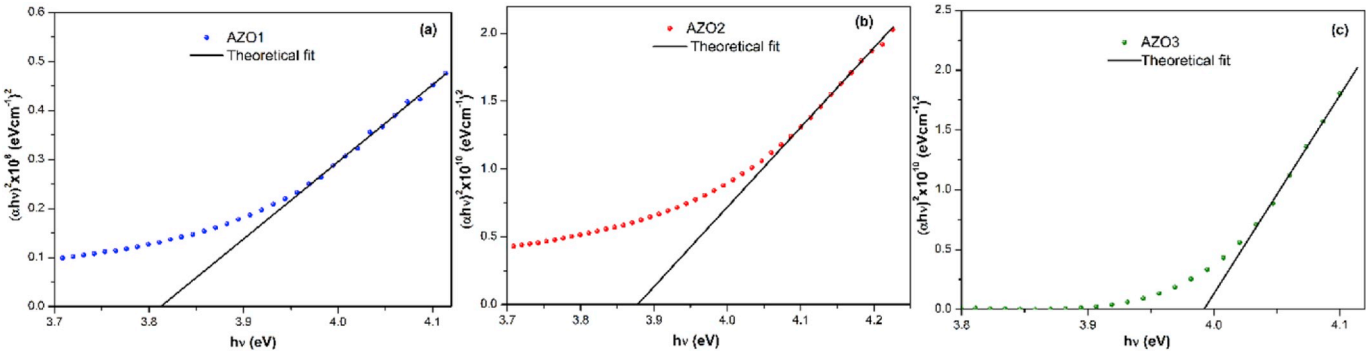


Fig. 3. $(\alpha h\nu)^2$ versus photon energy $(h\nu)$ graphs of AZO thin films at (a) 80 °C (AZO1), (b) 90 °C (AZO2) and (c) 100 °C (AZO3) growth temperature.

3. Results and discussions

3.1. Structural properties

The XRD spectra of AZO thin films grown on glass substrate are given in Fig. 1(a) and (b). It was observed that the growth temperatures of AZO1 (80°C) and AZO2 (90°C) and also Al doping ratios of AZO4 (5%) and AZO2 (10%) have the amorphous structure, as seen in Fig. 1(a) and (b). The XRD spectra of the AZO3 and AZO5 thin films indicated the existence of polycrystalline structure with hexagonal wurtzite phase of ZnO (JPCDS Card No: 36–1451). The impurity secondary phase peaks were observed related to α-Al_2O_3 and zinc hydrate for all samples as observed in the previously reported AZO thin films [29]. As seen from Fig. 1(a) and (b), the crystallinity increased with increasing both growth temperature and Al doping. As seen from Fig. 2(a), the impurity phase peaks (α-Al_2O_3 and zinc hydrate) in as-grown thin film AZO4 were observed. ZnO phase was not observed at all annealed temperatures for AZO4 thin film. In addition, the peak of zinc hydrate phase disappeared at 300°C and 400°C annealing temperatures. The disappearance of the zinc hydrate phase may be due to the removal of hydroxide phase with increasing annealing temperature that is more common phenomena in chemically grown thin films. As seen from Fig. 2(b), α-Al_2O_3 and zinc hydrate impurity phase peaks in AZO2 thin film began to disappear with increasing annealing temperature. ZnO phase (002) was observed at 300°C annealing temperature and the peak intensity of the ZnO phase increased with increasing annealing temperature. The impurity phases began to disappear for AZO5 thin film, while ZnO phase increases significantly with increasing annealing temperature, as given in Fig. 2 (c). Moreover, the crystallinity of AZO5 thin film increased with increasing annealing temperature.

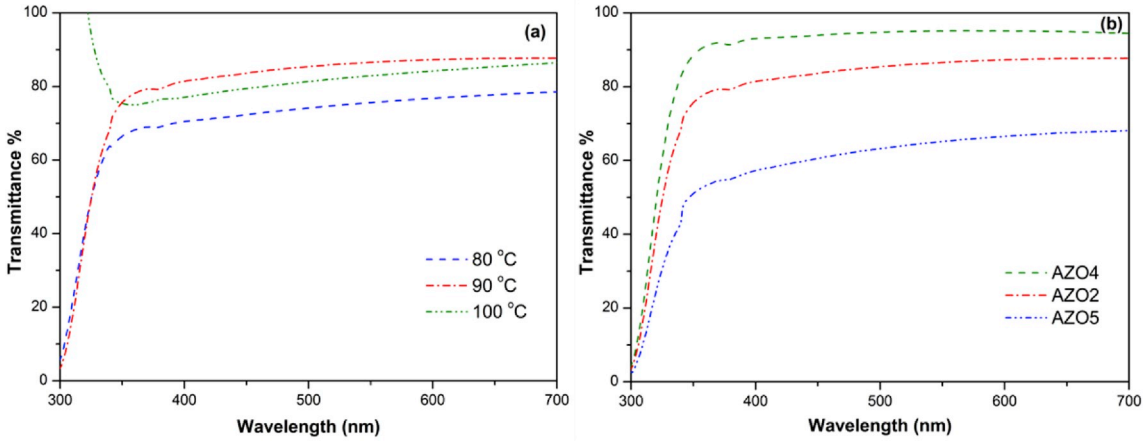


Fig. 4. Transmittance spectra of AZO thin films grown at (a) 80 °C, 90 °C, 100 °C growth temperature and (b) %5 (AZO4), %10 (AZO2), %20 (AZO5) Al doping ratios.

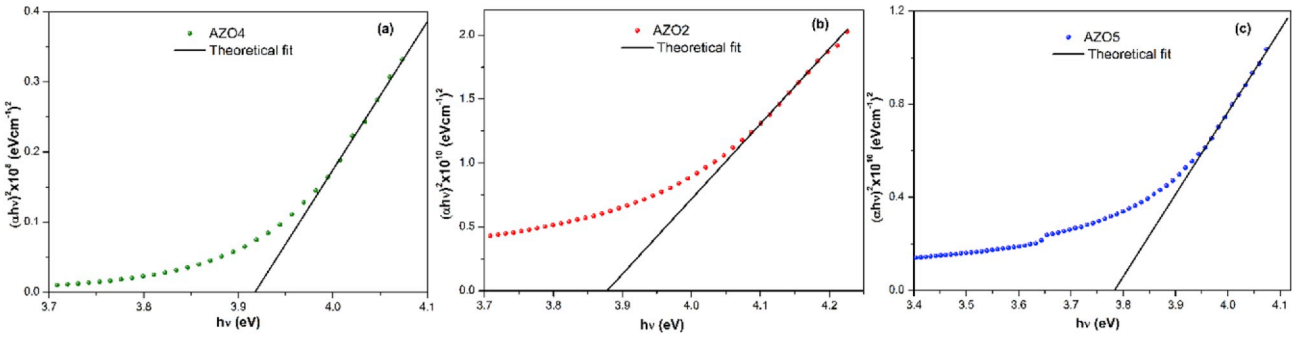


Fig. 5. $(\alpha hv)^2$ versus photon energy (hv) graphs of AZO thin films at (a) AZO4 (%5), (b) AZO2 (%10) and (c) AZO5 (%20) Al doping ratios.

3.2. Optical properties

The optical bandgap (E_g) for the AZO1, AZO2 and AZO3 thin films can be estimated from the following equation [34] by assuming a direct transition.

$$\alpha = \frac{A}{hv}(hv - E_g)^n \quad (1)$$

In above expression, A is a constant, E_g is the bandgap energy, v is the frequency of photon and n = 1/2, 2, 3/2, and 3 for direct allowed, indirect allowed, forbidden direct and indirect transitions, respectively. The energy bandgap of the studied films was obtained from the $(\alpha hv)^2$ versus photon energy (hv) graph as indicated in Fig. 3. The bandgap values of AZO1, AZO2 and AZO3 thin films are found to be 3.81, 3.87 and 3.99 eV, respectively. The fitting results indicate that the energy bandgaps increased with increasing growth temperature are attributed to decreasing defect states.

It can be seen from Fig. 4(a), AZO2 thin film grown at 90°C growth temperature shows better optical transmission than that of the other studied thin films. Therefore, nonlinear optical properties were studied for AZO thin films grown at 90°C. In order to investigate the doping effect on nonlinear absorption characteristics of ZnO thin films, AZO thin films were grown at 90°C growth temperature with different Al molar ratios. The transmittance spectra of AZO thin films at 5%, 10% and 20% Al molar ratios were shown in Fig. 4(b). As shown from Fig. 4 (b), the decreasing optical transmittance was observed in the visible region with increasing Al molar ratios. This is because of the increasing carrier concentration with increasing doping concentration [35].

The bandgap energies of AZO4, AZO2 and AZO5 thin films were found to be 3.91, 3.87 and 3.78 eV as shown in Fig. 5, respectively. The studied films have bigger band gap energies than the previously reported Al doped ZnO thin films [36–41]. The bandgap energy decreases with increasing doping concentration. Al behaves as a donor type material and supply more free electrons to the structure. Because of this, when the carrier concentration is surpassed over the Mott critical density in n-type semiconductor, the carrier-carrier and carrier-impurity interactions begin to dominate and cause to bandgap narrowing [42].

The nonlinear optical absorption was investigated by using OA Z-scan technique. The two-photon absorption (TPA), excited state absorption (ESA), free carrier absorption (FCA), nonlinear scattering processes or with the composition of these processes are responsible for the nonlinear absorption behavior in semiconductors [43]. The TPA is allowed process in semiconductor when the excited light energy is in between the bandgap energy (E_g) and $E_g/2$ [44]. In this work, the excited light energy equals to 2.33 eV which is in between (E_g) and $E_g/2$ of investigated thin films. Therefore, Eq. (2), which includes the contribution of OPA, TPA and FCA, was used as a fitting equation of open aperture Z-scan data.

$$\frac{dI}{dz'} = \frac{\alpha I}{1 + I/I_{sat}} - \frac{\beta_{eff} I^2}{1 + I^2/I_{sat}^2} = -f(I) \quad (2)$$

$$\alpha(I) = \alpha_0 + \beta I \quad (3)$$

where $\alpha(I)$ *is* the intensity dependent absorption and

$$\beta_{eff} = \beta + \left((\sigma_0 \alpha \tau_0)/\hbar\omega_0 \right) \quad (4)$$

where α_0 and β are the linear absorption coefficient and the nonlinear absorption coefficient, respectively. In Eq. (2), the first term is OPA and its saturation, while the second term is TPA and FCA and their saturations. In Eq. (4), σ_0 is the FCA cross-section and τ_0 is the pulse duration

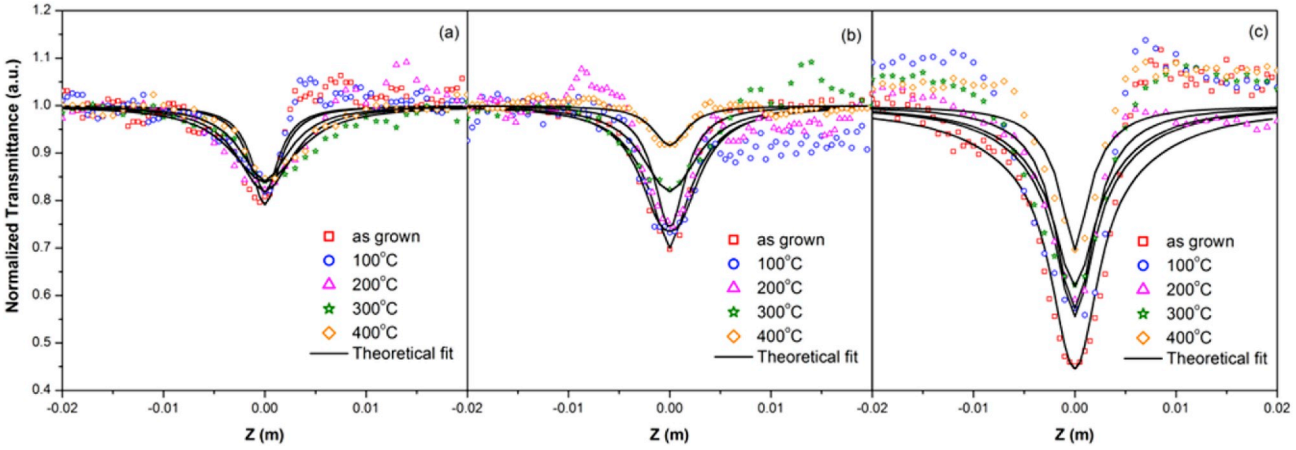


Fig. 6. Normalized transmittance of (a) AZO4, (b) AZO2 and (c) AZO5 thin films for 4 ns pulse duration with different annealing temperature at 532 nm wavelength ($I_o = 0.2$ GW/cm^2).

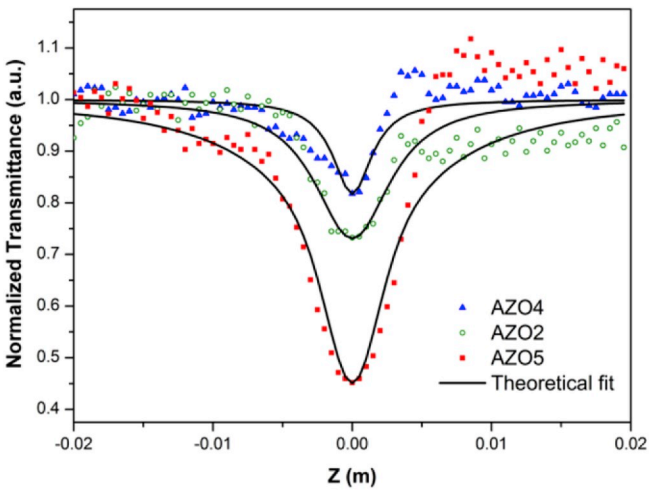


Fig. 7. Normalized transmittance of AZO thin films for 65 ps pulse duration at 532 nm wavelength ($I_o = 0.2\ GW/cm^2$).

Table 1
Nonlinear absorption coefficients of AZO thin films for nanosecond and picosecond laser excitation.

Sample	Nanosecond	I_{SAT} (GW/cm^2)	Picosecond	I_{SAT} (GW/cm^2)	Refs.
	β_{eff} (cm/W)		β_{eff} (cm/W)		
AZO4	1.34×10^{-4}	6.5	0.58×10^{-4}	15.3	Present work
AZO2	4.86×10^{-4}	8.2	1.81×10^{-4}	26.4	Present work
AZO5	6.12×10^{-4}	8.6	3.29×10^{-4}	39.8	Present work
2% AZO	5.8×10^{-5}	–	–	–	[48]
0.5%Mn doped ZnO nanorods	1.32×10^{-5}	–	–	–	[49]
Ag–ZnO nanowires	-2.42×10^{-8}	–	–	–	[50]

and ω_0 is the beam waist of the Gaussian spatial profiles at the focus. The Adomian decomposition method [45] provides a solution to the saturable problems for OA Z-scan theory [46]. Fitting details are given in the literature [1].

The experimental curves were fitted theoretically by using I_{SAT} and β_{eff} terms as free parameters (Eq. (2)). Figs. 6 and 7 show the theoretical fitting of OA Z-scan measurements corresponds to Eq. (2) for ZnO films with different Al concentration at 532 nm irradiation wavelength with 4 ns and 65 ps pulse durations, respectively. In the first term of Eq. (2), OPA contributes to SA due to defect states localized in bandgap and leads to saturation at low intensity threshold (I_{SAT}). The second term in Eq. (2) includes normalized transmittance signal originated from TPA and FCA saturation at high I_{SAT} values. OPA contribution is almost same for the same film thicknesses with nanosecond and picosecond pulse durations. The FCA contribution is effective in ns pulse duration, whereas the TPA contribution is dominant in ps pulse duration. Therefore, I_{SAT} values can be attributed to the TPA contribution in ps pulse duration, while OPA and FCA contribution in ns pulse duration. On the other hand, our experimental results showed that the I_{SAT} values increase with increasing Al doping ratio in ZnO thin films for both ns and ps pulse durations as seen in Table 1. Further, β_{eff} values are significantly affected by doping ratio and annealing process as seen in Tables 1 and 2. It is well known that the nonlinear absorption properties are strongly influenced from doping effect due to the increasing localized defect states [2]. The nonlinear absorption coefficients β_{eff} increase from 1.34×10^{-4} to 6.12×10^{-4} cm/W for 4 ns pulse duration with increasing of doping concentration due to increasing of localized defect states. The contribution of free-carrier absorption has significant influence on nonlinear absorption when the laser pulse duration at nanosecond and longer [47]. At the same peak irradiance, the longer pulses have larger energy so they create more free-carrier. Therefore, TPA induced FCA becomes dominant when longer pulses used. In order to observe the contribution of free-carrier absorption to nonlinear absorption at nanosecond regime, the OA Z-scan experiments were done at 65 ps pulse duration. The normalized transmittance curves are as shown in Fig. 7. The nonlinear absorption coefficient of AZO4, AZO2 and AZO5 are found to be 0.58×10^{-4}, 1.81×10^{-4} and 3.29×10^{-4} cm/W for 65 ps pulse duration at 0.2 GW/cm^2 input irradiance. As seen from Table 1, the β_{eff} values for ns pulse durations are bigger than the values for ps pulse durations at the same peak irradiance. This is because of the greater contribution of free-carrier absorption on nonlinear absorption at nanosecond pulse duration. The variation of nonlinear absorption coefficients with annealing temperature are depicted in Table 2. For comparison, we have also tabulated the values of nonlinear absorption coefficients of ZnO films. In our study, the values of nonlinear absorption coefficients are found to be at least an order of magnitude higher than the previously reported values, which are shown in Table 1 β_{eff} values decrease as the annaeling temperature increases found from OA *Z*-scan experiments. It is also found that for AZO films I_{SAT} values are bigger than that of annealed AZO films as expected due to the higher density of localized defect states. Our results indicated that the localized defect states decrease during annealing process.

4. Conclusion

AZO thin films grown at different growth temperature (80°C, 90°C and 100°C) and Al doping ratios (%5, %10 and %20) at 90 °C growth temperature by using the hydrothermal method were investigated to observe the effect of doping and annealing on nonlinear optical properties. The XRD measurements showed that the increasing growth temperature and the doping concentration could enhance the crystallinity of Al doped ZnO thin films. The transmittances were decreased from 90% to 55% with increased Al doping ratios. The bandgap energies increased from 3.81 eV to 3.99 eV with increasing growth temperature and decreased from 3.91 eV to 3.78 eV with increasing doping concentration. The nonlinear absorption coefficients increased from 1.34×10^{-4} to 6.12×10^{-4} cm/W and 0.58×10^{-4} to 3.29×10^{-4} cm/W with increasing doping ratios for both ns and ps pulse durations. The nonlinear absorption coefficients decreased with increase of annealing temperature due to the reduction of localized defect states during

Table 2
The nonlinear absorption coefficients of AZO thin films at different annealing temperatures for nanosecond laser excitation.

Annealing temperature	Nanosecond					
	AZO4		AZO2		AZO5	
	β_{eff} (cm/W)	I_{SAT} (GW/cm^2)	β_{eff} (cm/W)	I_{SAT} (GW/cm^2)	β_{eff} (cm/W)	I_{SAT} (GW/cm^2)
100 °C	1.25×10^{-4}	4.9	4.31×10^{-4}	6.3	5.17×10^{-4}	7.2
200 °C	1.21×10^{-4}	4.0	3.48×10^{-4}	4.8	4.10×10^{-4}	6.4
300 °C	1.15×10^{-4}	3.1	2.45×10^{-4}	4.2	3.72×10^{-4}	6.1
400 °C	1.00×10^{-4}	2.2	1.23×10^{-4}	3.6	2.45×10^{-4}	5.1

annealing process. Similar behavior was also observed for the saturation intensity threshold. Our results also showed that both nonlinear absorption coefficients and saturation intensity threshold can be changed by annealing and/or doping ratio.

Declaration of competing interest

The authors declare that they have no known competing financial interests or personal relationships that could have appeared to influence the work reported in this paper.

References

[1] M. Yuksek, U. Kurum, H.G. Yaglioglu, A. Elmali, A. Ates, J. Appl. Phys. 107 (2010).
[2] U. Kurum, M. Yuksek, H.G. Yaglioglu, A. Elmali, A. Ates, M. Karabulut, G. M. Mamedov, J. Appl. Phys. 108 (2010).
[3] A. Karatay, H.G. Yaglioglu, A. Elmali, M. Parlak, H. Karaagac, Opt. Commun. 285 (2012) 1471–1475.
[4] M. Shkir, A. Khan, A.M. El-Toni, A. Aldalbahi, I.S. Yahia, S. AlFaify, J. Phys. Chem. Solids 130 (2019) 189–196.
[5] P.M.R. Kumar, C.S. Kartha, K.P. Vijayakumar, T. Abe, Y. Kashiwaba, F. Singh, D. K. Avasthi, Semicond. Sci. Technol. 20 (2005) 120–126.
[6] M. Benhaliliba, C.E. Benouis, M.S. Aida, F. Yakuphanoglu, A.S. Juarez, J. Sol. Gel Sci. Technol. 55 (2010) 335–342.
[7] S.K. Hong, J.H. Lee, B.H. Cho, W.B. Ko, J. Ceram. Process. Res. 12 (2011) 212–217.
[8] A.B. Djurisic, X.Y. Chen, Y.H. Leung, A.M.C. Ng, J. Mater. Chem. 22 (2012) 6526–6535.
[9] Y.K. Tseng, C.J. Huang, H.M. Cheng, I.N. Lin, K.S. Liu, I.C. Chen, Adv. Funct. Mater. 13 (2003) 811–814.
[10] M.S. Arnold, P. Avouris, Z.W. Pan, Z.L. Wang, J. Phys. Chem. B 107 (2003) 659–663.
[11] M. Law, L.E. Greene, J.C. Johnson, R. Saykally, P.D. Yang, Nat. Mater. 4 (2005) 455–459.
[12] S. Liang, H. Sheng, Y. Liu, Z. Huo, Y. Lu, H. Shen, J. Cryst. Growth 225 (2001) 110–113.
[13] Q. Wan, Q.H. Li, Y.J. Chen, T.H. Wang, X.L. He, J.P. Li, C.L. Lin, Appl. Phys. Lett. 84 (2004) 3654–3656.
[14] M.H. Huang, S. Mao, H. Feick, H.Q. Yan, Y.Y. Wu, H. Kind, E. Weber, R. Russo, P. D. Yang, Science 292 (2001) 1897–1899.
[15] B.X. Lin, Z.X. Fu, Y.B. Jia, G.H. Liao, J. Electrochem. Soc. 148 (2001) G110–G113.
[16] S. Kim, G. Nam, H. Park, H. Yoon, S.H. Lee, J.S. Kim, J.S. Kim, D.Y. Kim, S.O. Kim, J.Y. Leem, Bull. Korean Chem. Soc. 34 (2013) 1205–1211.
[17] Y.H. Liu, S.J. Young, L.W. Ji, T.H. Meen, C.H. Hsiao, C.S. Huang, S.J. Chang, Ieee T Electron Dev 61 (2014) 1541–1545.
[18] F.C. Romeiro, J.Z. Marinho, A.C.A. Silva, N.F. Cano, N.O. Dantas, R.C. Lima, J. Phys. Chem. C 117 (2013) 26222–26227.
[19] Y.M. Liu, T. Wang, X. Sun, Q.Q. Fang, Q.R. Lv, X.P. Song, Z.Q. Sun, Appl. Surf. Sci. 257 (2011) 6540–6545.
[20] P. Banerjee, W.J. Lee, K.R. Bae, S.B. Lee, G.W. Rubloff, J. Appl. Phys. 108 (2010).
[21] D.Y. Zhang, K. Uchida, S. Nozaki, J. Appl. Phys. 118 (2015).
[22] O. Makuku, F. Mbaiwa, T.S. Sathiaraj, Ceram. Int. 42 (2016) 14581–14586.
[23] S.U. Offiah, S.N. Agbo, P. Sutta, M. Maaza, P.E. Ugwuoke, R.U. Osuji, F.I. Ezema, J. Solid State Electrochem. 21 (2017) 2621–2628.
[24] M. Berruet, C.J. Pereyra, G.H. Mhlongo, M.S. Dhlamini, K.T. Hillie, M. Vazquez, R. E. Marotti, Opt. Mater. 35 (2013) 2721–2727.
[25] J.L. Chen, J. Chen, D. Chen, Y. Zhou, W. Li, Y.J. Ren, L.L. Hu, Mater. Lett. 117 (2014) 162–164.
[26] X. Yu, X.M. Yu, J.J. Zhang, Z.Y. Hu, G.S. Zhao, Y. Zhao, Sol. Energy Mater. Sol. Cells 121 (2014) 28–34.
[27] Y. Ammaih, A. Lfakir, B. Hartiti, A. Ridah, P. Thevenin, M. Siadat, Opt. Quant. Electron. 46 (2014) 229–234.
[28] H. Kim, M. Osofsky, S.M. Prokes, O.J. Glembocki, A. Pique, Appl. Phys. Lett. 102 (2013).
[29] N.R. Yogamalar, A.C. Bose, J. Alloy. Comp. 509 (2011) 8493–8500.
[30] R. Vinodkumar, I. Navas, S.R. Chalana, K.G. Gopchandran, V. Ganesan, R. Philip, S. K. Sudheer, V.P.M. Pillai, Appl. Surf. Sci. 257 (2010) 708–716.
[31] A. Antony, S. Pramodini, P. Poornesh, I.V. Kityk, A.O. Fedorchuk, G. Sanjeev, Opt. Mater. 62 (2016) 64–71.
[32] K.M. Sandeep, S. Bhat, S.M. Dharmaprakash, P.S. Patil, K. Byrappa, J. Appl. Phys. 120 (2016).
[33] G.P. Bharti, A. Khare, Opt. Mater. Express 6 (2016) 2063–2080.
[34] J.I. Pankove, Optical Process in Semiconductors, second ed., Dover Publications, New York, 1971.
[35] T.C. Damen, S.P.S. Porto, B. Tell, Phys. Rev. 142 (1966) 570.
[36] K.D.A. Kumar, S. Valanarasu, V. Ganesh, M. Shkir, S. AlFaify, H. Algarni, J. Mater. Res. 33 (2018) 1523–1533.
[37] K.D.A. Kumar, S. Valanarasu, V. Ganesh, M. Shkir, A. Kathalingam, S. Alfaify, J. Electron. Mater. 47 (2018) 1335–1343.
[38] K.D.A. Kumar, V. Ganesh, M. Shkir, S. AlFaify, S. Valanarasu, J. Mater. Sci. Mater. Electron. 29 (2018) 887–897.
[39] M. Arif, M. Shkir, S. AlFaify, V. Ganesh, A. Sanger, H. Algarni, P.M. Vilarinho, A. Singh, J. Mater. Res. 34 (2019) 1309–1317.
[40] K.D.A. Kumar, S. Valanarasu, S.R. Rosario, V. Ganesh, M. Shkir, C.J. Sreelatha, S. AlFaify, Solid State Sci. 78 (2018) 58–68.
[41] K.D.A. Kumar, V. Ganesh, S. Valanarasu, M. Shkir, I. Kulandaisamy, A. Kathalingam, S. AlFaify, Mater. Chem. Phys. 212 (2018) 167–174.
[42] S.C. Jain, J.M. Mcgregor, D.J. Roulston, J. Appl. Phys. 68 (1990) 3747–3749.
[43] P.G.L. Frobel, S.R. Suresh, S. Mayadevi, S. Sreeja, C. Mukherjee, C.I. Muneera, Mater. Chem. Phys. 129 (2011) 981–989.
[44] R. Boyd, Nonlinear Optics, third ed., Elsevier, Amsterdam, 2008.
[45] B. Gu, Y.X. Fan, J. Wang, J. Chen, J.P. Ding, H.T. Wang, B. Guo, Phys. Rev. A 73 (2006).
[46] B. Gu, Y.X. Fan, J. Chen, H.T. Wang, J. He, W. Ji, J. Appl. Phys. 102 (2007).
[47] E.C. Fox, H.M. Van Driel, Ultrashort Processes in Condensed Matter, Springer, New York, 1993.
[48] K.M. Sandeep, S. Bhat, S.M. Dharmaprakash, Opt. Laser. Technol. 102 (2018) 147–152.
[49] A. Singh, S. Kumar, R. Das, P.K. Sahoo, RSC Adv. 5 (2015) 88767–88772.
[50] U. Vinoditha, B.K. Sarojini, K.M. Sandeep, B. Narayana, S.R. Maidur, P.S. Patil, K. M. Balakrishna, Appl Phys a-Mater 125 (2019).